SANDIA REPORT

SAND2018-1007
Unlimited Release
Printed January 2018

Separability of Mesh Bias and Parametric Uncertainty for a Full System Thermal Analysis

Benjamin Schroeder, Humberto Silva III and Kyle D. Smith

Prepared by
Sandia National Laboratories
Albuquerque, New Mexico 87185 and Livermore, California 94550

Sandia National Laboratories is a multimission laboratory managed and operated by National Technology and Engineering Solutions of Sandia, LLC., a wholly owned subsidiary of Honeywell International, Inc., for the U.S. Department of Energy's National Nuclear Security Administration under contract DE-NA0003525.

Issued by Sandia National Laboratories, operated for the United States Department of Energy by National Technology and Engineering Solutions of Sandia, LLC.

Available to DOE and DOE contractors from
U.S. Department of Energy
Office of Scientific and Technical Information
P.O. Box 62
Oak Ridge, TN 37831

Telephone: (865) 576-8401
Facsimile: (865) 576-5728
E-Mail: reports@adonis.osti.gov
Online ordering: http://www.osti.gov/bridge

Available to the public from
U.S. Department of Commerce
National Technical Information Service
5285 Port Royal Rd
Springfield, VA 22161

Telephone: (800) 553-6847
Facsimile: (703) 605-6900
E-Mail: orders@ntis.fedworld.gov
Online ordering: http://www.ntis.gov/help/ordermethods.asp?loc=7-4-0#online

SAND2018-1007
Unlimited Release
Printed January 2018

Separability of Mesh Bias and Parametric Uncertainty for a Full System Thermal Analysis

Benjamin Schroeder
V&V, UQ, Credibility Processes

Humberto Silva III
Thermal Sciences & Engineering

Kyle D. Smith
Analytical Structural Dynamics

Sandia National Laboratories
P.O. Box 5800
Albuquerque, NM 87185-9999

Abstract

When making computational simulation predictions of multi-physics engineering systems, sources of uncertainty in the prediction need to be acknowledged and included in the analysis within the current paradigm of striving for simulation credibility. A thermal analysis of an aerospace geometry was performed at Sandia National Laboratories. For this analysis a verification, validation and uncertainty quantification workflow provided structure for the analysis, resulting in the quantification of significant uncertainty sources including spatial numerical error and material property parametric uncertainty. It was hypothesized that the parametric uncertainty and numerical errors were independent and separable for this application. This hypothesis was supported by performing uncertainty quantification simulations at multiple mesh resolutions, while being limited by

resources to minimize the number of medium and high resolution simulations. Based on this supported hypothesis, a prediction including parametric uncertainty and a systematic mesh bias are used to make a margin assessment that avoids unnecessary uncertainty obscuring the results and optimizes computing resources.

Acknowledgment

We would like to acknowledge our funding sources, W78 Systems - Thermal Computational Simulation and Advanced Simulation and Computing - Full System Modeling. We would also like to thank our SAND report peer reviewers Nicholas Francis and Kevin Dowding, project peer reviewers Kenneth C. Chen, Linda K. Jones, Brantley Mills, Ryan M. Keedy, Brian Carnes, Nicholas Francis, and Ethan T. Zepper, and informal peer reviewers of the project Tre Shelton, Roy E. Hogan Jr., Walter R. Witkowski, Kevin Dowding, and James T. Nakos.

Contents

Appendix

List of Figures

Chapter 1

Introduction

This document is meant to compile a verification, validation and uncertainty quantification (VVUQ) workflow applied to a thermal modeling analysis performed at Sandia National Laboratories (Sandia). In order to facilitate circulation of the VVUQ methods, ideas, and approach used during the thermal analysis, the specific application and model inputs will not be described and predictions will be normalized. It is hoped that the complexities faced in this problem, even when presented in a generic format, will resonate with other thermal analysts, and that lessons learned from this work can be shared.

1.1 Background on Thermal Application

The system of interest can be described in general terms as a transient, large scale, three-dimensional, aerospace system experiencing a specific thermal environment. Coupled physics being modeled within the analysis include thermal conduction, thermal convection, radiation, phase change, and chemistry. A significant limitation for this analysis is the scale of the computation. The simulation is calculated using a finite element formulation with the SIERRA Thermal/Fluids code [30], where the simulation's nominal mesh contains over 1.5 million four-node tetrahedral (tet4) elements. Within the limitations of available parallel-computing computational resources, it takes on the order of hours to run a simulation using the nominal mesh and days to run the simulation for more refined meshes.

The prediction or quantity of interest (QoI) for this analysis was the timing of a thermal race. A thermal race is the difference in time between two events occurring when a system is exposed to a thermal environment. Thermal races are common thermal analysis QoIs within Sandia's thermal analyst community [7]. Typically, thermal races are tracked due to requirements that one event must occur prior to another event in order to make safety assertions. Figure 1.1 illustrates the type of thermal race being studied for the current analysis. For this analysis we are interested in discrete events occurring at different locations in the system and in the time between those two event occurring. Our system has a requirement that event 1 must occur prior to event 2; and we need to assess margin in the system's ability to meet that requirement.

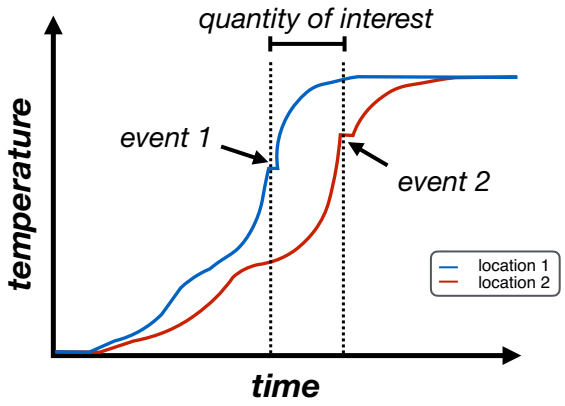

Figure 1.1: Concept of thermal race used for this analysis

1.2 Computational Simulation Credibility

A major area of emphasis within Sandia's computational analysis communities is establishing the credibility of a simulation prediction. One approach towards establishing prediction credibility being advocated is the use of the Predictive Capability Maturity Model (PCMM) [18]. PCMM breaks a computational simulation analysis into six elements: representation and geometric fidelity, physics and material model fidelity, code verification, solution verification, model validation, and uncertainty quantification (UQ) and sensitivity analysis. Credibility of a computational simulation is established through PCMM by ranking the maturity level achieved for each analysis element. For each element many subelements are specified by PCMM and the maturity level of the element is then determined by which and to what extent those subelements are completed. For instance, a subelement of the UQ and sensitivity element is to perform a sensitivity analysis. Different extents of accomplishing this element include not performing a sensitivity analysis, perform a precursory qualitative sensitivity analysis, and performing a rigorous quantitative sensitivity analysis. Computational simulation credibility is not considered as a binary score for this analysis, credible or not credible, but as an evidence package transparently communicating uncertainties, assumptions, and limitations.

Our thermal modeling analysis VVUQ workflow, base on PCMM elements, is shown in Figure 1.2. One additional aspect of a this VVUQ workflow for thermal analyses not included in PCMM, is margin assessment. PCMM is typically used to support simulation predictions, while margin assessment supports decision making. Within thermal analyses, margin assessment acts as the link and communication tool between thermal analysts and decision makers (customers), clearly making it a necessary element of a VVUQ workflow.

A high level overview of the VVUQ workflow follows. When representing a real-world system with a finite element representation, simplifications such as removing screws or wires, known as defeaturing, is common. Similarly, when specifying the physics and material models that will be

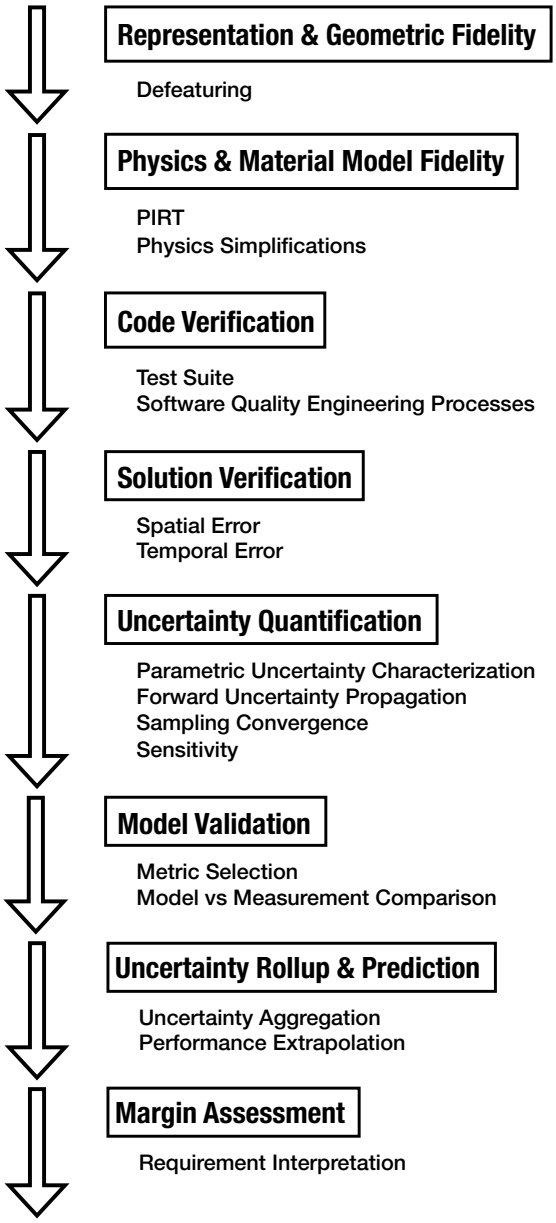

Figure 1.2: Typical VVUQ workflow applied to thermal analyses

used to represent a complex engineering system, simplifications to the set of physics being solved, such as ignoring the movement of material as it softens, is common. When enacting simplifications to the fidelity of the representation and geometry or the physics and material models, the impact on the prediction of interest should be considered. When analyzing the physics and material model fidelity, a tool known as the phenomena identification and ranking table (PIRT), can be used to identify important gaps [37, 36]. To ensure that the physics models have been correctly translated to the code, code verification activities such as test suites and software quality practices are necessary. Numerical schemes are used to discretize our thermal systems of interest. Use of numerical schemes results in numerical errors in the simulation predictions such as spatial and temporal er-

rors, which can be quantified for the application of interest using solution verification methods. Within thermal system models are many uncertain parameters (material properties, boundary conditions, initial conditions) that need to be characterized and that uncertainty propagated through the model to provide estimates of prediction uncertainty. When applying forward uncertainty propagation approaches, it must be ensured that the resulting prediction distribution is sufficiently resolved for the application questions of interest. Computational models used for thermal analyses generally contain simplifications that result in model form errors. In order to characterize model form errors, comparison with experimental data, also known as model validation, is necessary. When performing validation comparisons, metrics need to be specified and adequacy of the model's performance for the predictions of interest assessed. So far, various errors and uncertainties from different sources have been analyzed within the workflow, but ultimately they must be aggregated and applied to the prediction of interest. This aggregation process is known as uncertainty rollup [28]. Often, a method of extrapolating the aggregated uncertain and knowledge about model form error must be applied in order to make predictions in the application space of interest. A common goal for thermal analyses is to make margin assessments or compare predicted performance against system requirements. This comparison must also consider the uncertainty present in the simulation and potentially in the requirement definition.

Because of the project's scope and institutional limitations, not all elements of PCMM are presented herein. Evaluation of the representation and geometric fidelity as well as the physics and material model fidelity are not presented within this document so as to not elaborate on details about the specific application. Within Sandia's analysis structure, code verification is primarily the responsibility of the code development teams; the code teams use software quality engineering (SQE) processes and test suites to ensure reliable, reproducible results and numerical algorithm verification tests to check algorithm implementation. Further details about code verification will be neglected within the document. For the thermal analysis reported upon within this document, no experimental data was available, so model validation was not able to be considered. An example of a model simplification used that may result in model form error when conducting this thermal analysis is neglecting structural mechanics phenomena that may occur as a result of thermal loads applied to metal based engineering systems. To avoid the additional computational costs of integrating the thermal simulation with a structural mechanics simulation, modeling simplifications of the structural impact are incorporated into the thermal simulation. Without model validation to characterize model form uncertainty, it is difficult to estimate the impact of this uncertainty source on the prediction of interest. Because many elements of PCMM are not reported within this document, a full simulation credibility assessment will not be considered. Instead, the VVUQ analysis workflow is used to provide a credible analysis structure, that may eventually use all aspects of PCMM to provide predictions with confidence in our understanding of their credibility.

One aspect of element maturity shared by all elements within PCMM is peer review. At the end of this project, a formal presentation based peer review was conducted, resulting in a slide deck, comments from reviewers, and responses to those comments. To take the peer review process further, a generic version of the analysis is being presented in this document to provide a more in-depth peer review of the VVUQ process, methods, and interpretation of results. Additionally, it is hoped that credibility of subsequent thermal analyses can be improved by providing lessons learned that can be leveraged.

1.3 VVUQ Workflow Applied to Application

Given the aforementioned caveats to our PCMM based approach, we can now provide a more detailed account of the VVUQ workflow applied to the thermal analysis problem of interest. The first step to any VVUQ based approach must be to define the analysis objectives and available resources. Analysis objectives are required upfront because they are necessary to define the scope and types of VVUQ activities necessary. Available resources often limit what VVUQ activities are possible. The objective of this analysis is to characterize the margin and uncertainty present in our prediction of a thermal race. Limitations to the analysis include financial and computational budget as well as a timeframe. Given an objective and limitations, the necessary elements of the VVUQ workflow are selected and enacted.

Solution verification is performed using different mesh refinements to characterize the simulation's spatial discretization bias trend. Parameter uncertainty descriptions are then assigned to uncertain material properties and propagated through the simulation using a sampling based approach to provide an ensemble of predictions characterizing the impact of input uncertainties in the prediction space. The statistical convergence of the forward uncertainty propagation is then assessed with relevant metrics. Using information from the uncertainty propagation and input uncertainty definitions, model sensitivity is assessed indicating which material property uncertainty sources are most significant for the analysis. Next, the dependence of the mesh bias and parameter uncertainties is assessed, those uncertainty sources are rolled-up, and a total prediction uncertainty is determined. Comparing the total prediction uncertainty against the system's performance requirement results in a margin assessment, allowing further decisions about the continued work on the project to be determined.

When performing computational simulations of physical engineering systems, aggregating heterogenous errors and uncertainties is necessary. Often, the impact of one uncertainty source is studied, but in order to make credible predictions, the greater effort required to aggregate multiple sources is necessary. Previously at Sandia, many pieces of the full rollup problem have been considered independently: the rollup of information from multiple validation points to the prediction conditions of interest [10], embedding model discrepancy into model parameter uncertainties during calibration to make better extrapolative predictions [29], and calibration of model parameters from multiple levels of model complexity using Bayesian networks [33]. Other methods of integrating uncertainty from different sources (i.e. calibration and validation) have been academically studied. Solution verification and sampling uncertainty for a fluids simulation application was investigated [20]. [21] considered validation, uncertainty quantification, experimental input and output data error sources. Combining parameter calibration and model validation is a particularly tricky situation for which many different approaches have been presented [12, 15]. ASME's standards committees have published approaches toward uncertainty rollup [34, 35] that provide conservative methods towards aggregating uncertainties from the many sources present in simulations.

The present work takes a novel approach towards rolling up mesh bias and parametric uncertainty to make margin estimations, where being informative and reducing uncertainty is valued over conservatism. To increase the interpretability of prediction uncertainty, this approach aims to

maintain separability of uncertainty sources in the prediction space and to test the interdependence of the uncertainty sources. Establishing the dependence of the uncertainty sources upon other uncertainty sources, allows the prediction uncertainty to be reduced (as compared to the typical situation where dependence must be assumed due to not proving otherwise).

The remainder of this document will be structured as follows. First, the VVUQ methods for all aspects of the VVUQ workflow considered for this analysis are described in chapter 2. Next, the analysis results for those same VVUQ workflow elements are reported in chapter 3. Significant issues and findings of this analysis are discussed in chapter 4. Finally, conclusions, ideas for continued study, and possible paths forward are provided in chapter 5.

Chapter 2

Methods

2.1 Application Physics

Our model is first spatially semi-discretized using a second-order Galerkin finite element method, and then temporally discretized using finite differences [32, 31]. We then solve the transient energy conservation equation including thermal diffusion, enclosure radiation, bulk convection, and chemical kinetics, as described in greater detail within Appendix A, for each subdomain of our discretized problem. To solve equations in time an implicit, second-order accurate, backward finite difference 2 (BDF2) with adaptive time stepping is applied. The solution time step is often limited by the chemical kinetics, which are solved using the CHEMEQ library [38]. CHEMEQ uses a stiff ordinary differential equation integrator and the resulting time steps are often smaller than those required by the thermal solve alone. The thermal time step is not set to the chemical time step, but is not allowed to be greater than a specified multiple of the chemical time step.

2.2 Solution Verification

Because numerical spatial and temporal discretization schemes are used to solve the system of equations applicable to our application, the numerical errors associated with the numerical methods must be considered. To quantify the numerical error impacting the predictions of interest, an a posteriori mesh refinement method [19] known as Richardson extrapolation will be used [22]. The relation between the 'exact' solution and the predicted solution is [25]

$$f_{h,\Delta t} - f_{\text{exact}} = Ah^p + B\Delta t^q + \mathscr{O}(h^{p+1}) + \mathscr{O}(\Delta t^{q+1}). \tag{2.1}$$

Here h represents the spatial discretization, Δt represents the temporal discretization, $f_{h,\Delta t}$ is the predicted value for the current spatial and temporal discretization, f_{exact} is the solution to the equations without any numerical error, A and B are multiplicative constants on the error terms, p and q are the respective orders of convergence, and $\mathscr{O}$ are higher order errors. For this study we assume that our discretization is sufficient to place our solution in the asymptotic range, implying that higher order error terms have significantly smaller values than the main error terms and thus can be removed from our equation describing numerical error. In previous thermal analyses we have performed solution verification for a variety of numerical error sources including mesh resolution and numerical solver tolerances (e.g. chemistry step multiplier, residual norm tolerance,

predictor-corrector tolerance, etc.). Those previous studies, which considered different but related QoIs, found mesh resolution to be the dominant numerical error source. To support our assumption that other numerical error sources contribute minimally to the current study, the tightest numerical solver tolerance settings previously considered are used in the current study. Neglecting temporal error is an assumption commonly made within our thermal analysis community and stems from using adaptive time-stepping with tight tolerances and many prior analyses that found minimal impact of the time step size on the thermal analyses' results.

Removing the higher order and temporal errors from the numerical error equations results in

$$f_h - f_{\text{exact}} = Ah^p. \tag{2.2}$$

Now to estimate the spatial discretization error present in a simulation, three parameters need to be solved for: A, p, and f_{exact}. To solve for these three unknowns, Equation (2.2) can be evaluated for three different mesh discretization.

$$\begin{aligned} f_1 &= f_{\text{exact}} + Ah_1^p \\ f_2 &= f_{\text{exact}} + Ah_2^p \\ f_3 &= f_{\text{exact}} + Ah_3^p \end{aligned} \tag{2.3}$$

Ratios describing the relative change in discretization between the three different meshes can be specified as

$$\begin{aligned} r_{1,2} &= h_2/h_1 \\ r_{2,3} &= h_3/h_2. \end{aligned} \tag{2.4}$$

To simplify solving for the unknown parameters, uniform mesh refinement (UMR) can be implemented, where the spatial discretization is cut in half for each subsequent mesh, resulting in 8 and 64 times more elements than the nominal mesh.

$$r_{1,2} = r_{2,3} = r = 2 \tag{2.5}$$

Solving for the unknown parameters with (2.3)-(2.5) yields

$$p = \frac{\ln(\frac{f_3 - f_2}{f_2 - f_1})}{\ln(2)} \tag{2.6}$$

$$f_{\text{exact}} = f_1 + \frac{f_1 - f_2}{2^p - 1} \tag{2.7}$$

$$A = (f_i - f_{\text{exact}})/h_i^p. \tag{2.8}$$

Once p, A and f_{exact} have been calculated, estimates of the mesh bias for any grid within the spatially asymptotically converging region can be made via

$$\text{Mesh Bias} = f_i - f_{\text{exact}} = Ah_i^p. \tag{2.9}$$

Applying the aforementioned solution verification methodology to the application problem of interest comes with assumptions, simplifications, and recognized issues. Assumptions required by traditional Richardson extrapolation are: asymptotic range, uniform mesh spacing, systematic mesh refinement, smooth solutions, and discretization error being the dominant numerical error source [19]. When neglecting higher order error terms, we assumed that our simulation was in the asymptotic range. To test this assumption additional mesh refinements would have been required, but this was not deemed cost appropriate for the analysis. Uniform element sizes are not typically feasible for thermal analyses of interest within the Sandia thermal analysis community. The meaning of h is unclear for meshes containing a wide distribution of element sizes. To avoid the complexity of the mesh size distribution, the discretization length scale is applied as a relative refinement ratio from the original mesh. Uniform mesh refinements are used and the predictions of interest are considered smooth; satisfying two Richardson extrapolation assumptions. From previous thermal analyses we have found that other numerical error sources such as temporal discretization and iterative solves provide errors of significantly smaller impact than the error due to the mesh resolution. The thermal race QoI is a local quantity, while the applied solution verification method was formulated for global quantities. Considering the potential impact of these assumptions, it is clear that there will be uncertainty in the resulting numerical error estimates. This uncertainty is acknowledged, but quantifying the magnitude of this uncertainty source is not currently possible or feasible. Multiplying the estimated mesh bias by engineering safety factors, which were developed based on knowledge gained from applications in specific engineering domains, has been advocated as a means of providing conservative estimates [24]. Instead, we will treat the calculated mesh bias as a best estimate and acknowledge that epistemic uncertainty (lack of knowledge) exists both above and below the calculated value exists [23]. All assumptions made in solution verification are noted here for transparency and so that they may be absorbed into the assessment of simulation credibility.

2.3 Uncertainty Quantification

After the initial solution verification, the analysis shifts focus to estimating the impact of parametric uncertainty on the prediction. A benefit of performing solution verification prior to characterizing parametric uncertainty effects is that solution verification can illuminate simulation construction issues prior to consuming computational resources on running parametric studies. If no major simulation formulation issues are found during solution verification, the analysis can continue forward. Initial physical intuition for the system of interest can also be gained from the solution verification studies such as identifying the dominant thermal pathways.

UQ is the effort to characterize the impact of uncertain parameters on the prediction of interest. Many thermal engineering simulations are created using deterministic codes. In order to estimate the uncertainty associated with a prediction, making the prediction stochastic, parameter uncertainties are propagated forward through the deterministic simulations, resulting in an ensemble of predictions. Typical uncertain parameters for thermal analyses include material property values, initial conditions, and boundary conditions. Another common type of uncertainty specific to model validation activities is the uncertainty in where measurements occurred (location or time epistemic

measurement error). The current analysis was restricted to material thermal properties as uncertain parameters.

All uncertain material properties present in the system of interest must be defined. Different mathematical descriptions of parameter uncertainty are available including probabilistic, interval, possibilistic, and belief and plausibility. Choosing which type of description to use to describe parameter uncertainties depends on what type of uncertainty is being described and what tools are available to handle propagation of the uncertainty descriptions through the model.

For this analysis a probability distribution is specified to described each uncertain parameter. Following common practice within the Sandia thermal analysis community, truncated normal distributions are used for thermal conductivity, density, and specific heat parameters, and triangular uncertainty distributions are used for emissivities. The width of each distribution is specified relative to the level of comfort in specifying property values for the specific material; well known materials have less spread in their uncertainty distributions than less well known materials. The system being studied contains hundreds of parts and many of the parts are constructed from the same type of material, so the question of what to consider as an uncertain variable arises.

When dealing with systems comprised of many parts, some of which are composed of the same material type (i.e. stainless steel or aluminum), different approaches towards assigning uncertain parameters exist. One option, known as part-centric, is to treat each material property of each part as an uncertain parameter. Another option, material-centric, is to treat each material property as an uncertain parameter and then use that same uncertain parameter value for each part that is composed of that material. The tradeoff between these two uncertainty assignment approaches is the number of uncertain parameters included in the analysis versus forcing correlation between parts composed of the same material. It can be argued that complete independence of material properties for parts composed of the same materials may be incorrect due to the likelihood that the same base material was used to create many parts. An argument against assuming full correlation is that some parts composed of 'material A' may have a significant impact of the prediction, while other parts made of that material may have no impact, yet only a single sensitivity for that uncertain parameter will be quantified.

Instead of either of those extremes, a combined part- and material-centric approach is taken. This combined part- and material-centric approach tries to optimize the number of uncertain parameters explored by exploiting knowledge of the dominant thermal path gained from the solution verification study, while also allowing for sensitivity to specific parts to be identified. Based on the knowledge of the dominant thermal path, material properties in each part along that thermal path are treated as uncertain parameters (part-centric) and for the rest of the system all materials composed of the same materials share uncertain material property values (material-centric). For instance, if a part (part 5) along the dominant thermal path is composed of stainless steel, then the thermal properties of stainless steel (specific heat $C_{P,SS,5}$, thermal conductivity $\kappa_{SS,5}$, and emissivity $\varepsilon_{SS,5}$) for that part are each an uncertain parameter. Then all other parts in the system made of stainless steel, but not along the dominant thermal path, share the same uncertain thermal properties (specific heat $C_{P,SS,all}$, thermal conductivity $\kappa_{SS,all}$, and emissivity $\varepsilon_{SS,all}$).

The uncertainty descriptions used to characterize parameter uncertainties potentially describe

both epistemic uncertainty (our lack of knowledge) and aleatory uncertainty (true variability). Ideally epistemic and aleatory uncertainty sources would be separately specified and kept separated throughout the analysis. If a prediction is presented with segregated uncertainty, it allows the amount of prediction uncertainty that could be reduced with further effort to be identified. Segregated prediction uncertainty also provides an indication of the true variability expected in the performance characteristic of interest. Separation of epistemic and aleatory uncertainty is not feasible for this and many similar analyses, where parameter uncertainty descriptions with separated uncertainties are not available, and separate propagation of the uncertainty types through the model is not computationally affordable. If computational cost was not a limiting factor, double looped sampling methods like second order probability [4] could be used to maintain separation of uncertainty types during forward uncertainty propagation. A consequence of the inability to separate the uncertainty sources is that the prediction uncertainty must be interpreted as representing an aggregation of true variability and our lack of knowledge about parameter values. Not all parameters are believed to have natural variability. For parameters without natural variability, the uncertainty descriptions are purely epistemic (reducing down to a true value with sufficient knowledge).

Many thermal properties are specified as functions of temperature. For functional material parameters (x_i), uncertainty is assigned as a scaling factor, e.g.,

$$x_i = (m_i T + b_i) \times \text{Scaling Factor}. \tag{2.10}$$

Here m and b are material specific values and this functional form is represented in a tabulated format for many materials. For temperature dependent thermal properties this uncertainty assignment method is believed to be realistic due to the increased difficulty in measuring such properties at higher temperatures.

To propagate parameter uncertainty forward through the model, Latin hypercube sampling is used. Latin hypercube sampling [8] is used for forward uncertainty propagation due to its relative simplicity, flexibility to use any number of samples, and ability to provide statistical prediction estimates at a lower computational cost than Monte Carlo random sampling. For an uncertainty propagation study that can afford n samples with p uncertain parameters, a p dimensional hypercube is formed where each dimension spans the uncertainty range of the respective parameter and each dimension is stratified into n equally probable partitions or bins. In two dimensions this can be easily visualized as a 2-D grid where the x axis represents one variable and the y axis represents the other variable. The n samples are then randomly placed throughout the p dimensional grid, but for each parameter only one sample can be placed in each of its partitions. Figure 2.1 shows one possible instance for a four sample LHS study and the mapping of equal probably partitions of each parameter space from the uncertain parameter CDFs into the LHS hypercube. LHS insures coverage of the uncertainty space of all uncertain parameters, relatively independent of the number of samples used.

Issues with sampling based uncertainty quantification include the high number of samples necessary to converge prediction characteristics and determining when enough samples have been taken to provide sufficiently converged prediction characteristics. The number of samples required is dependent on how many of the uncertain parameters are driving the total uncertainty. A priori it is difficult to know if 20 or 20,000 samples will be required, so a means of assessing convergence

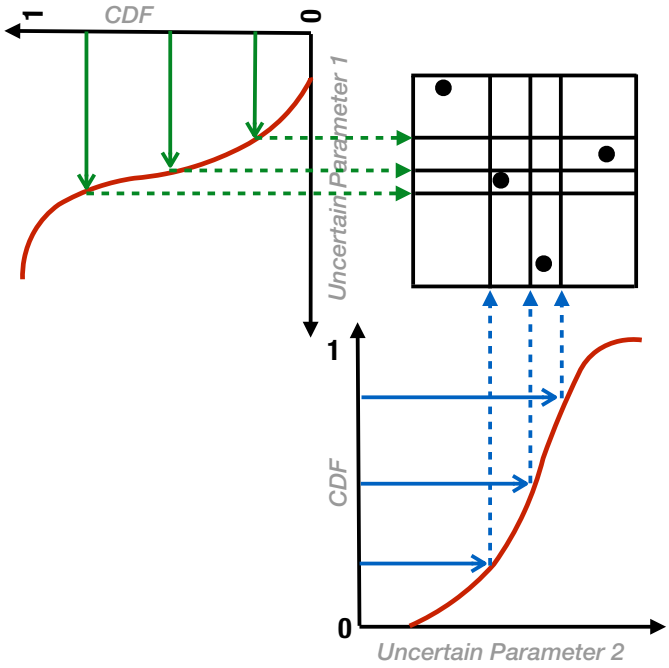

Figure 2.1: Illustration of equal probable stratification for a 2-D, four sample LHS study

is necessary. To help assess convergence, a variant of LHS known as incremental LHS (iLHS) can be used [26]. iLHS provides increments where each subsequent increment builds off the previous increment (uses the same points), but increases the total number of sample points. Each increment constitutes a full LHS study and can be used to provide statistical estimates of the prediction distribution. Then by comparing the prediction results between increments, convergence can be assessed. The Dakota software package [1] contains the iLHS implementation used for this analysis. The iLHS algorithm available in Dakota doubles the number of samples for each increment. An illustration of two steps of an iLHS study where the sample size doubles from four to eight is shown in Figure 2.2.

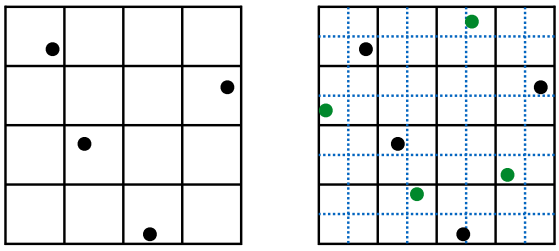

Figure 2.2: Illustration of an increment of iLHS where a 2-D, four sample LHS study is updated to an eight sample study

2.4 Sensitivity Analysis

Beyond strictly making the prediction of interest, thermal analyses are often interested in determining which parameter uncertainties have the greatest impact on the prediction uncertainty, also known as sensitivity. Sensitivity information provides physical insights into complex simulations as well as guidance on which additional experiments/research could have the greatest impact on this type of prediction (resource allocation). To gather this type of sensitivity information, global sensitivity measures are needed. For this analysis Pearson correlation coefficients (ρ) will be used as the global sensitivity metric.

$$\rho_i = \frac{\sum_{i=1}^{n}(x_i - \overline{x})(y_i - \overline{y})}{\sqrt{\sum_{i=1}^{n}(x_i - \overline{x})^2 \sum_{i=1}^{n}(y_i - \overline{y})^2}} \tag{2.11}$$

Here x are the input parameter values, y are the corresponding simulation output values, n is the number of samples, and the bar notation indicates a mean value.

The use of Pearson correlation coefficients as a sensitivity measure requires a few assumptions: a linear relationship between model parameters and predictions, continuous variables, all variables being normally distributed, and homoscedasticity (prediction uncertainty maintains the same spread across the linear trend). Assuming a linear relationship between inputs and outputs of thermal models is typically perceived to be a safe assumption. While not all of the parameter uncertainties for this analysis are normally distributed, they are all symmetric and bounded, so it is assumed that this should not have a significant impact on the correlation results. Application simulation predictions are never truly normally distributed, but approximating them as such is believed to be a reasonable assumption for sensitivity calculations.

Pearson correlation coefficient values are between -1 and 1, where the magnitude indicates the strength of the linear relationship and the sign indicates positive or negative correlation. Squared Pearson correlation coefficients indicate the percent of the prediction (y) uncertainty caused by the uncertainty in parameter (x) if the underlying assumptions hold. An equivalent way of thinking about the squared Pearson correlation coefficients is as the r^2 value from a simple linear least squares fit. Comparing the difference between the sum of the squared coefficients and unity, estimates the fraction of the prediction variance explained by assuming a linear relationship between the inputs and output, or the strength of the linear assumption. If the sum of the squared coefficients is judged to be sufficiently close to unity, the interpretation of the squared coefficients as the percent of prediction uncertainty caused by that parameter's uncertainty can be used. This interpretation of the correlation coefficients requires an assumption that interactions between input parameters cause an insignificant amount of uncertainty in the prediction. Otherwise, if the assumptions are not sufficiently met or the summed squared correlation coefficients are judged not close enough to unity, the correlation coefficient should be treated as a qualitative measure of sensitivity.

If the linear assumption for sensitivity was found to be incorrect (a significant amount of the prediction variance is not captured), another global sensitivity metric that makes less restrictive assumptions about the form of the relationship between model inputs and outputs could be used. An example of such a sensitivity measure is Sobol indices [27]. Sobol indices for the interaction

effect of multiple input parameters can also be calculated for systems where this impact is believed to be significant, further reducing required assumptions.

2.5 Uncertainty Rollup and Prediction

When making predictions, all uncertainty sources need to be included. For this analysis the relevant uncertainty sources are the spatial discretization error and parameter uncertainty. Other uncertainty/error sources potentially included in the uncertainty rollup for other analyses might include model form uncertainty resulting from validation activities, other numerical errors such as the temporal discretization error, and uncertainties due to extrapolating the model beyond ranges where data is available. So far section § 2.2 characterized a mesh bias estimate using nominal parameter values and section § 2.3 characterized the forward propagation of material property uncertainties through the model using the nominal mesh. In reality, the simulation's total error needs to account for both uncertainty/error sources and the interaction between those sources has not been quantified.

$$f(\mathbf{X},h) - f_{\text{exact}}(\mathbf{X}) = Ah^p \tag{2.12}$$

Here $\mathbf{X}$ are the uncertain input parameters and h is the spatial discretization.

One possible assumption that would allow the prediction's total uncertainty to be quantified is that the impact of the parametric uncertainty and mesh bias are independent.

$$f(\mathbf{X},h) = f(\mathbf{X}) + f(h) = f_i(\mathbf{X}) \tag{2.13}$$

This assumption can be tested by running the UQ simulations at different mesh resolutions.

$$f(\mathbf{X},h_i) - f_{\text{exact}}(\mathbf{X}) = f(\mathbf{X},h_j) - f_{\text{exact}}(\mathbf{X}) \tag{2.14}$$

If the UQ prediction distribution is the same for different mesh resolutions, the independence of mesh bias and parameter uncertainty would be established. Establishing independence of uncertainty/error sources allows for the total prediction uncertainty to be estimated.

$$f_i(\mathbf{X}) - f_{\text{exact}}(\mathbf{X}) = Ah_i^p \tag{2.15}$$

Although independence could be quantified through sufficient sampling, we are limited by our computational resources, so we must minimize the number of simulation runs conducted for the higher mesh resolutions. Instead of running all UQ samples at multiple mesh resolutions, only a subset of the samples are run at the higher mesh resolutions. For the current problem we hypothesize that propagating the tails of the UQ prediction distribution to the higher mesh resolutions can be used to establish that the two sources of uncertainty/error are sufficiently independent with respect to the QoI (our thermal race margin estimate). To enact this approach, the parameter values that resulted in the two extreme tail values of the prediction distribution for the nominal mesh are then used to make predictions for both of the more resolved meshes. If the spread between the tail samples is relatively constant as a function of mesh resolution, this will be used as evidence of independence and allow the mesh bias and parameter uncertainty to be rolled-up into a total uncertainty estimate.

2.6 Margin Assessment

For thermal system analyses, a typical goal is to predict system performance in order to estimate a performance margin. Margin questions typically originate from a customer of the thermal analysis, meaning that the customer defines the prediction quantity of interest (QoI) and specifies a performance requirement. At Sandia this type of margin question is frequently framed in a quantification of margin and uncertainty (QMU) [6, 9] framework. The basic formulation of a QMU type presentation is to provide a visual of the performance distribution, requirement, margin between the performance distribution and requirement, and uncertainty in the performance distribution. The exact definitions of margin and uncertainty depend on the type of performance measure being considered and type of uncertainty present in the prediction. For some applications the difference between the mean performance and the requirement is considered the margin, and uncertainty is the standard deviation of the performance distribution (K-factors) [16]. Other applications consider the distance between an extreme tail percentile of the performance distribution (0.01 percentile would be an example of a extreme tail percentile for Figure 2.3) and the requirement as the margin and the uncertainty in the percentile estimate due to data sparsity as the uncertainty (tolerance interval) [16].

For the current application, the margin question of interest is the proximity of the performance distribution to the requirement. To quantitatively describe this margin question, we will use the percent of predictions violating the requirement as the margin assessment, and the spread in the prediction distribution as the uncertainty in this assessment. Figure 2.3 illustrates the definitions of margin and uncertainty used for the current comparison of a performance prediction and a requirement. This margin and uncertainty designation is deemed appropriate when the prediction

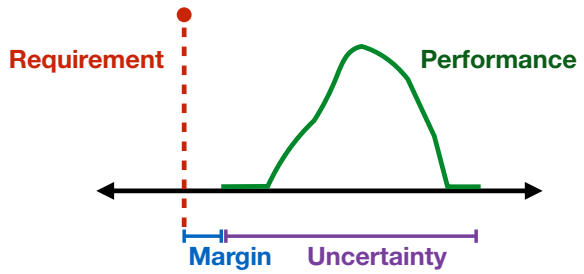

Figure 2.3: Conceptual illustration of margin assessment comparing predicted performance and a requirement. Margin is defined as distance from edge of the prediction distribution to the requirement and uncertainty is defined as total prediction distribution spread.

distribution largely represents epistemic uncertainty, or when the true value could be anywhere within the distribution. In this approach the margin quantifies the worst case possibility within our current understanding (smallest difference between requirement and predicted behavior in performance space) and the uncertainty quantifies our lack of knowledge about the situation.

Chapter 3

Results

3.1 Solution Verification

Following our VVUQ workflow (Figure 1.2), solution verification of the prediction QoI is first calculated using nominal values for uncertain material parameters. Two uniform mesh refinements are performed ($\circ$), allowing order of convergence and an extrapolated true value ($\times$) to be calculated with (2.6)-(2.7). Figure 3.1 shows the solution convergence and Richardson extrapolation results. The QoI prediction appears to be convergent with refinement of the mesh resolution and the observed order of convergence is 1.04. This convergence rate is below the second order convergence expected for the second order spatial discretization scheme being solved for the thermal system, but is anticipated due to the many assumptions absorbed in the solution verification approach described in section § 2.2.

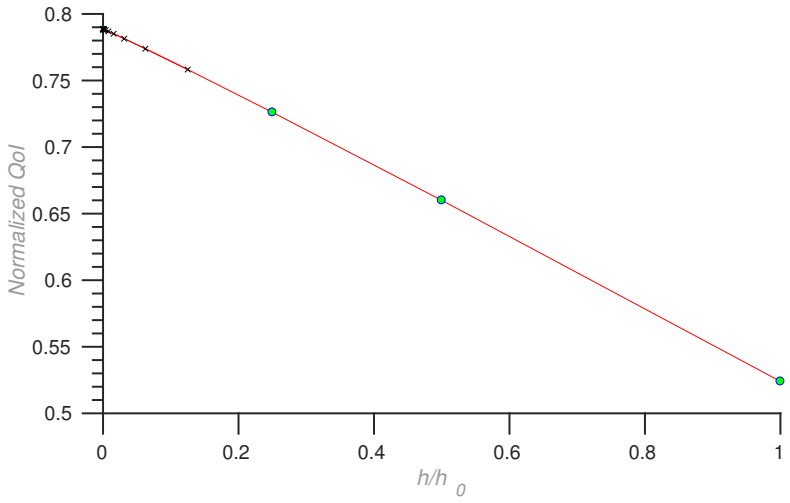

Figure 3.1: Application of Richardson extrapolation to UMR mesh convergence study. Predicted QoI values for different mesh refinements are shown as blue dots and black $\times$ markers indicate Richardson extrapolations for possible additional uniform mesh refinements. Mesh refinements are shown as values normalized by the nominal mesh.

Using the extrapolated 'true' value (0.79) as the reference point for determining the best esti-

mate of mesh bias for other mesh resolutions is shown as blue bars in Figure 3.2. Using the mesh

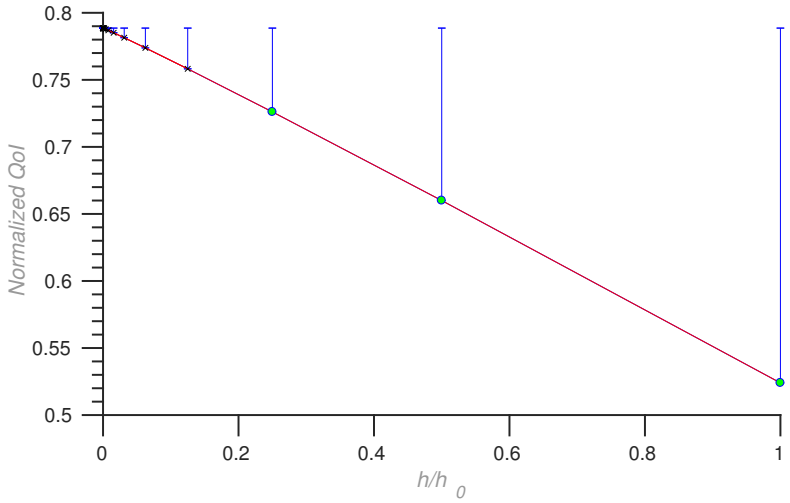

Figure 3.2: Defining mesh bias as difference between QoI prediction at each mesh resolution and Richardson extrapolated QoI prediction. Blue bars are added to Figure 3.1 to indicate the magnitude of mesh bias present for different mesh refinements.

bias definition specified by (2.9), results in a significant bias (-0.27) being present in simulations calculated at the nominal ($h/h_0 = 1$) mesh.

3.2 Uncertainty Quantification: Forward Propagation

Next, uncertain material parameters in the simulation are specified. For this thermal system analysis around 150 uncertain material property parameters are defined for our combined part- and material-centric approach. Propagating parameter uncertainties through the simulation using iLHS, results in QoI prediction distributions, as shown in Figure 3.3. Increments of samples sizes 20, 40, 80, 160, 320, and 640 are used. Normal distributions are fit to the simulation results to test the common normality assumption, but the distributions appear to show negative skew. Comparing the QoI prediction distributions based on 320 and 640 samples shows that the distributions appear roughly converged, but metrics are needed to quantify the sampling convergence in terms of the prediction questions of interest.

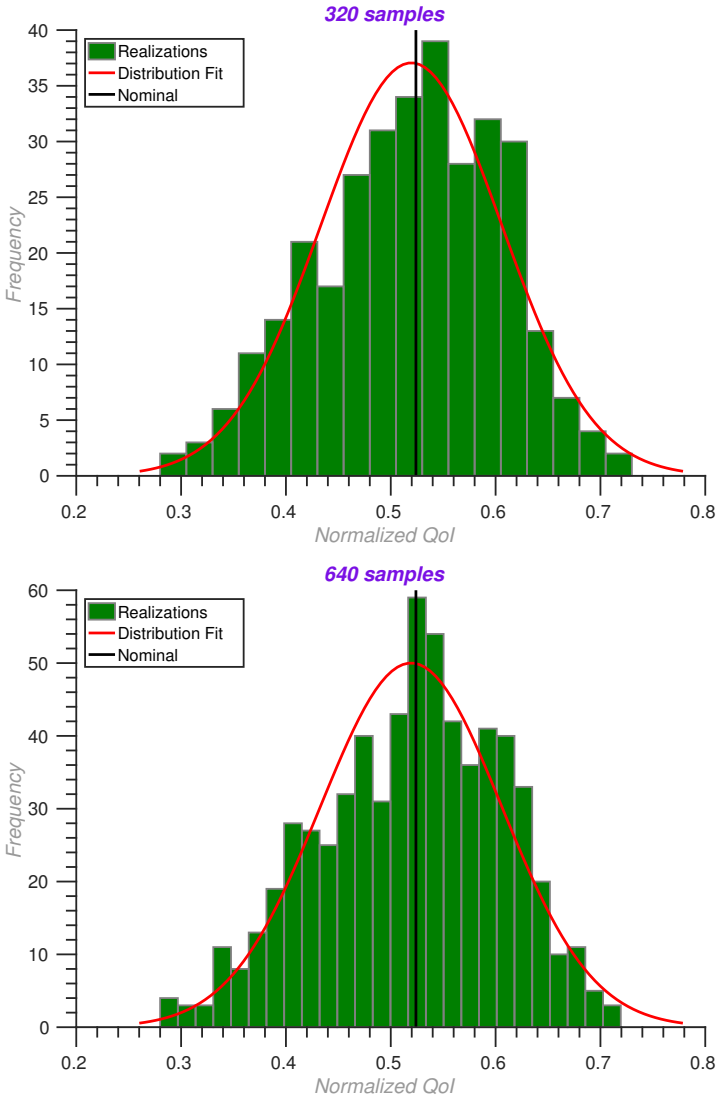

Figure 3.3: Histograms of QoI predictions based on 320 and 640 samples. Normal distributions fit to the sample mean and standard deviation are shown as red lines.

3.3 Sensitivity Analysis

One of the analysis prediction questions of interest is which parameter uncertainty definitions have the greatest impact on the prediction, or sensitivity. For this analysis Pearson correlation coefficients (2.11) are used as the sensitivity metric. The top three Pearson correlation coefficients, where correlation is between the simulation QoI predictions and the values of specific material parameters, are shown for iLHS sample sizes of 320 and 640 in Figure 3.4. Comparing the correlation coefficients based on the two incremental sample sizes indicates that the ordering and relative magnitude of the sensitivity measure has converged. The ordering and magnitudes of all parameter sensitivities have not converged using 640 samples, but the magnitude of the first two parameters indicates that understanding the sensitivity to the remaining parameters is inconsequen-

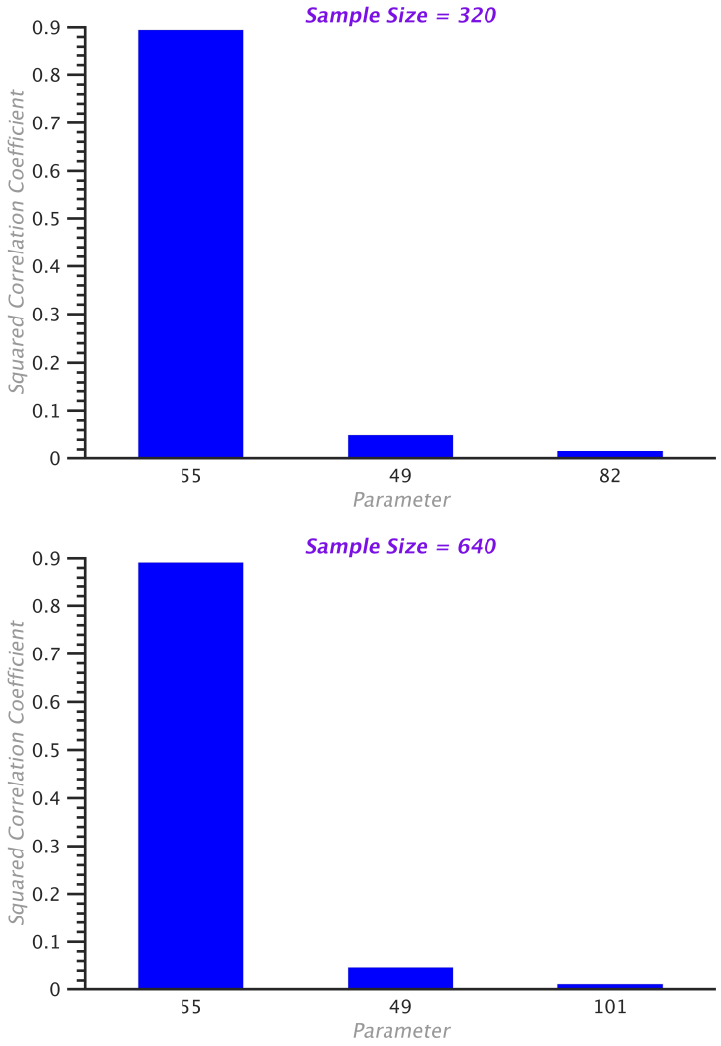

Figure 3.4: Top three squared Pearson correlation coefficients based on 320 and 640 iLHS samples, where correlation is between uncertain material parameters and QoI predictions

tial. It appears that uncertain parameter 55 is the dominant source of uncertainty for making the desired QoI prediction. The sum of the squared correlation coefficients determines the linearity of the relationship between model inputs and outputs. The sum of all squared correlation coefficients is approximately 1.0, indicating that a linear assumption when quantifying sensitivity is able to account for 100% of the prediction variance, assuming that the impact of interactions between parameters contributes an insignificant amount of uncertainty. This interpretation of the sensitivity results allows the analyst to make the quantified conclusion that parameter 55 accounts for 89% of the QoI prediction uncertainty. This sensitivity study shows that refinement of the nominal definition of parameter 55 could have a significant impact on the simulation prediction results and reduction of the uncertainty characterization of parameter 55 would significantly reduce the prediction uncertainty.

3.4 Uncertainty Quantification: Sampling Convergence

To assess if enough samples of the uncertain input parameters have been propagated through the model, or if the prediction distribution has converged with respect to the questions of interest, convergence criteria are defined. For the prediction of interest we chose the prediction distribution mean, the prediction distribution standard deviation, the total spread of the prediction distribution, and the magnitude of the leading Pearson correlation coefficient, shown in Figure 3.5, as metrics of convergence. The four criteria (ϕ) for sampling convergence are plotted as relative error versus

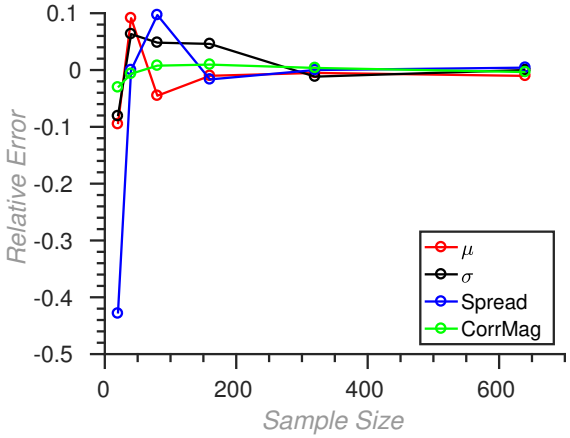

Figure 3.5: Four metrics of sampling convergence: relative error value of the mean of the predicted QoI distribution (μ), the standard deviation of the predicted QoI distribution (σ) , the distance between the minimum and maximum samples of the predicted QoI distribution (Spread), and the magnitude of the leading correlation coefficient (CorrMag).

sample size, where relative error is the difference between the criteria's value at the last sample size ($n/2$) and the current sample size (n), normalized by the current sample size's value.

$$\text{Relative Error} = \frac{\phi_n - \phi_{n/2}}{\phi_n} \tag{3.1}$$

It appears that using 320 samples sufficiently converged the specified criteria, but the results from 640 samples provide greater confidence in this conclusion. Even after 160 samples less than 6% changes in ϕ values is observed.

We choose these four convergence criteria for this problem because they are representative of the analysis questions of interest. Because the sensitivity to input parameters was sought, the magnitude of the leading correlation coefficient was selected as a convergence criteria to provide credibility to the sensitivity conclusion. The margin between the prediction distribution and the requirement was another major analysis concern, so we sought to ensure convergence of the prediction distribution's total spread. Then when making margin assessments, uncertainty in the prediction must also be considered, so the prediction distribution's mean and standard deviation are included as criteria for convergence. Ensuring these four convergence criteria are met supports the credibility of analysis statements build upon those same values (prediction leading sensitivity sources, mean, standard deviation, and spread).

3.5 Uncertainty Rollup and Prediction

Now that the impact of mesh bias and forward propagation of parametric uncertainty have been characterized independently, the hypothesis that they can be treated as independent uncertainty sources, when aggregated to make a prediction for this analysis, can be tested. To test this hypothesis, the parameter sets that resulted in the minimum and maximum predictions (or left and right ends of the prediction distribution) are used with meshes once and twice uniformly refined. If the hypothesis of independence of mesh bias and parametric uncertainty is true, the spread of the prediction distribution should be insensitive to mesh discretization. Figure 3.6 shows simulation results for the left extreme, nominal, and right extreme of the prediction distribution (specified by the nominal mesh results) as a function of grid resolution. From the figure it appears that the

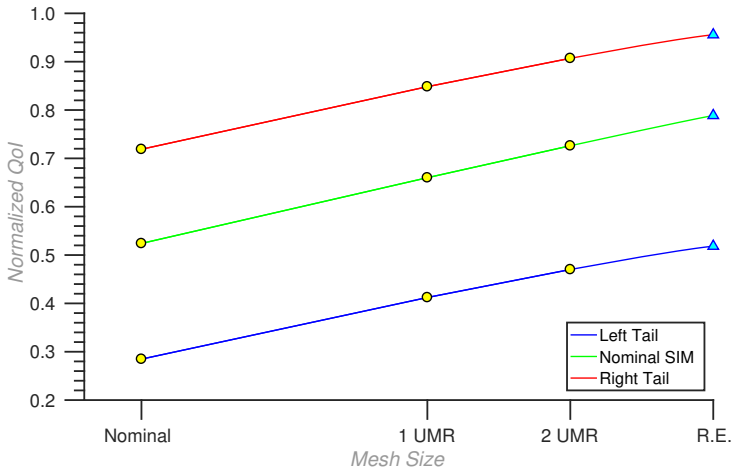

Figure 3.6: Impact of mesh size on QoI prediction for simulations that produced the nominal, left extreme, and right extreme values of the QoI prediction distribution for the nominal mesh. Yellow circles indicate simulation results and blue triangles are Richardson extrapolated values.

prediction distribution's spread is relatively insensitive to the mesh resolution.

To further investigate the relationship between the prediction distribution's spread and the mesh resolution, the trend and Richardson extrapolation of the distribution's spread is plotted in Figure 3.7. The figure shows a converging trend in the distributional spread, but the magnitude of the mesh bias impact on the distribution's spread is only 0.3% of the extrapolated value (or 0.003 in QoI units). This dependence is considered insignificant for the predictions of interest due to the disparity in the magnitudes of impacts. The analysis results have shown a mesh bias of roughly -0.27 QoI units and parametric uncertainty causing a 0.44 QoI unit spread. These bias and uncertainty values are notable for this analysis because it is commonly assumed within our thermal analysis community that parametric uncertainties dominate the total uncertainty in predictions, yet for this analysis these terms are of similar magnitude. Based on these results, we go forward in the analysis with the assumption of independence and separability of mesh bias and parametric uncertainty.

Separable mesh bias and parametric uncertainties impacts allows for the two terms to be treated

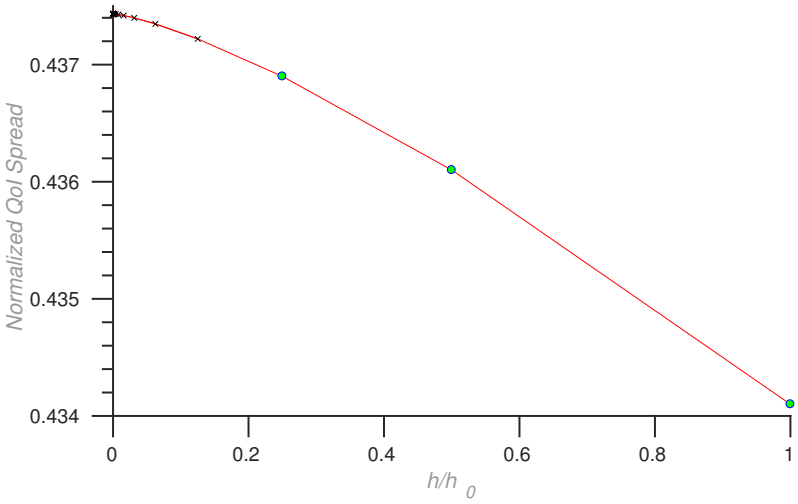

Figure 3.7: Richardson extrapolation applied to solution convergence of QoI prediction spread based on UMR samples. Blue dots indicate meshes used and black $\times$ markers are based on Richardson extrapolation for possible additional UMR meshes. Mesh refinements are shown as values normalized by the nominal mesh.

additively. To make predictions with respect to the margin question of interest, the prediction distribution calculated for the nominal mesh can be shifted by the mesh bias calculated for the nominal mesh, resulting in a prediction distribution that accounts for both sources of uncertainty. This shift of the prediction distribution is shown in Figure 3.8. When shifting the distribution,

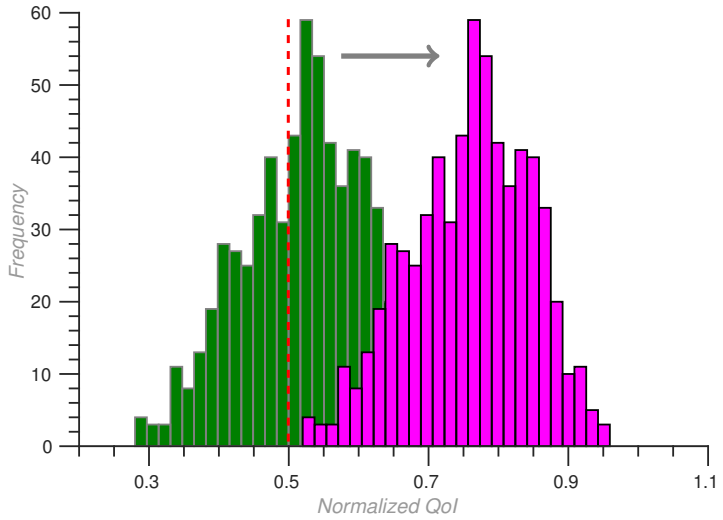

Figure 3.8: Shifting QoI histogram predicted using nominal mesh by the quantified mesh bias (gray arrow). Performance requirement (0.5) is shown as the red dashed line.

the mesh bias calculated for the left tail sample of the distribution is added to all iLHS predicted values.

3.6 Margin Assessment

For this analysis the performance requirement is that the predicted behavior be above 0.5 normalized QoI units. Shifting the QoI predicted distribution by the mesh bias results in a positive margin between the left tail of the prediction distribution and the performance requirement. Figure 3.9 shows how the percent of samples comprising the prediction distribution that are below the performance requirement scales with mesh resolution. Almost 40% of predictions are below the

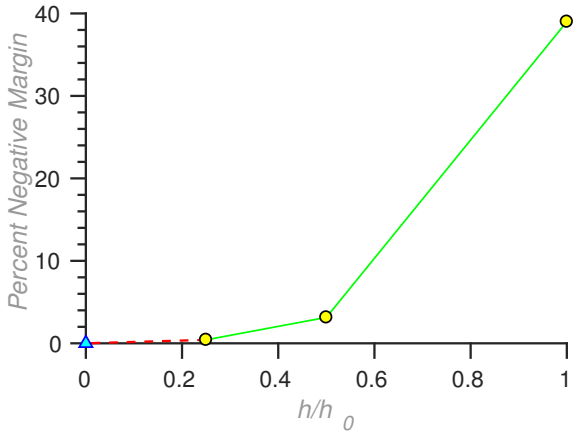

Figure 3.9: Percent of the prediction distribution below the performance requirement (0.5) as a function of mesh refinement. Percent values are based on the number of iLHS samples below the threshold. Yellow dots correspond to actual meshes tested and the blue triangle is based on the Richardson extrapolation estimate of the true value. Mesh refinements are shown as values normalized by the nominal mesh.

performance requirement if only parametric uncertainty is considered. As the impact of mesh bias for increasing levels of mesh refinement are taken into account, the percent of the prediction distribution below the threshold diminishes. If the Richardson extrapolated estimate of mesh bias is incorporated into the prediction, then none of the 640 iLHS samples is below the performance requirement. In terms of margin and uncertainty, the presented results are still concerning due to the margin over uncertainty (M/U) ratio being significantly less than 1. While the importance of the specific M/U value is debatable, having uncertainty in the prediction of a larger magnitude than the margin is concerning.

Chapter 4

Discussion

The approach presented for handling numerical and parameter uncertainty is the major VVUQ development resulting from this analysis. If the mesh bias and parametric uncertainty sources had not been shown to be separable, more conservative assumptions about their interaction would have been necessary. An example of a common approach towards providing a conservative prediction is to use engineering factors, which are multiplied by the identified uncertainty magnitudes to calculate the uncertainty value ultimately included with the prediction.

The analysis results found that accounting for the spatial discretization error as a mesh bias shifted the predicted performance distribution in a positive margin direction. Another way of thinking about this result is that the nominal mesh provided conservative estimates of performance. Neglecting mesh bias will not always provide a conservative performance estimate, which is only a result of the direction in which the simulation performance converges. For analyses that cannot afford additional uncertainty quantification simulations at higher mesh resolutions but whose solution verification studies show the nominal mesh to be conservative, this might be exploited to justify using results of nominal mesh, parametric studies as conservative performance estimates.

The numerical uncertainty identified within the simulation was characterized as a bias instead of an uncertainty. This was done for two reasons. First, the impact of the mesh resolution was clearly causing the nominal mesh simulation to be shifted to the left, resulting in a negative margin for the question of interest. Additionally, if the spatial discretization error was characterized as an uncertainty and that uncertainty was added to the parametric uncertainty, this would widen the prediction distribution, increasing the amount of negative margin. We acknowledge that the characterized mesh bias is only a best estimate of an epistemic uncertainty due to fitting the Richardson extrapolation with three points. Communicating that additional uncertainty factor when providing the simulation prediction allows the decision maker to determine its impact on their own analyses. If that epistemic uncertainty source was aggregated into the simulation prediction by the thermal analyst, the decision maker would be presented with a more conservative, but less informative result.

The uncertainty characterizations produced to describe the uncertainty in material thermal properties were largely epistemic. Some of the material properties may contain natural variability due to manufacturing processes or different sources of the material, but it is generally believed that the magnitude of those variabilities is significantly less than our lack of knowledge about the true parameter value. This means that the prediction distribution is also largely epistemic in nature,

which motivated our choice of margin assessment. The true prediction value could be anywhere within the prediction distribution, so we characterized margin as the worst case simulation evaluation. Uncertainty in this margin assessment was then our epistemic uncertainty about the true margin value. If the uncertainty in the prediction distribution had been largely aleatory, it would have been more reasonable to think of margin differently. In a prediction dominated by aleatory uncertainty, the uncertainty reflects possible instances of the margin, any of which could occur; the margin may then be defined as the most probable possible margin. Communicating the correct interpretation of the prediction's margin assessment can have a significant impact on a decision maker's conclusions.

Ultimately, the margin assessment showed that minimal margin exists for the analysis question of interest. The current simulations found positive margin, but when also accounting for the epistemic uncertainty in the mesh bias value, there is likely some portion of the prediction distribution with negative margin. If the margin had been found to be significantly larger, both in value and relative to the uncertainty in the prediction, then decision makers may not have needed to consider the epistemic uncertainties associated with the prediction. Finding that minimal margin exists versus finding a significant portion of negative margin may result in different courses of action by a decision maker, so the approach taken towards aggregating uncertainty/error sources was impactful for this analyses. The sensitivity results indicate that further study of parameter 55 may provide significant aid to making a decision based on the current analysis.

The present analysis indicates that our understanding of performance margin is clouded by our lack of knowledge. If parameter 55's uncertain characterization had represented true natural variability in a material property, then the performance distribution would have represented the probability of minimal margin existing. The difference in interpretation for decision makers is our lack of knowledge indicates that minimal margin exists versus minimal margin exists with a certain likelihood.

We have decided to think of computational simulation credibility as a framework to specify objectives, enact VVUQ methods, and report assumptions, limitations, and results. To establish the credibility of the work present within this document, we leveraged a VVUQ workflow largely based on the elements of PCMM. Not all elements of the workflow were reported within this document due to institutional limitations and project scope, but all were mentioned to provide a reference of what we considered a full workflow. Through documenting assumptions absorbed into the VVUQ analysis elements, working through elements in an integrated fashion, and orienting all elements towards the project's question of interest, customers should have greater clarity in how the analysis results can be leveraged for their decision making process.

Chapter 5

Conclusions

Like all projects with finite scope and resources, many questions remain and were left for future work. The work presented provides a detailed account of a real engineering thermal analysis, structured in a VVUQ workflow in order to progress towards providing a means of communicating simulation credibility to a customer. Using PCMM elements as the analysis components, the assumptions and performance of the simulations are able to be concisely communicated. A novel approach towards aggregating numerical uncertainty and parametric uncertainty was presented. Through providing evidence that numerical and parametric uncertainty sources were independent, they were able to be aggregated additively as an uncertainty plus bias. Future work may consider additional simulation evaluations at a medium mesh resolution, allowing the generation of a surrogate model. A medium resolution surrogate model could then be compared against all evaluations at the lower mesh resolution, providing greater evidence of the dependence between parametric and numerical uncertainty sources, while still limiting the number of costly fine resolution evaluations. Interpretation of prediction uncertainty as being primarily epistemic or aleatory in nature has a significant impact on the interpretation of a margin assessment and should be communicated to decision makers.

Appendix A

General Description of Physics Equations Solved

Heat Conduction

The mathematical description used to describe heat conduction in a stationary material region (Ω) is

$$\rho C \frac{\partial T}{\partial t} = \frac{\partial}{\partial x_i}\left(k_{ij}\frac{\partial T}{\partial x_j}\right) + Q \tag{A.1}$$

where ρ is the material density, C the specific heat, k_{ij} the thermal conductivity tensor, Q the volumetric heat source, t the time, x_i the spatial coordinates and T the temperature [3]. Materials can be be heterogeneous with the conductivity tensor being at most orthotropic [2]. Material properties can take functional forms with dependence on time, spatial location, chemical composition, and/or temperature. Energy release from chemical reactions is included in the variation of Q, which can take on the same tensor form as the other additive terms in (A.1). When enclosure radiation is coupled with heat conduction all other pertinent field variables can take on specified material dependencies.

Enclosure Radiation

Enclosure radiation is modeled using the net-radiation method as described in [11]. Associated with each surface is a uniform temperature T_j, an area A_j and a surface emissivity ε_j. An energy balance for each surface in the enclosure leads to the following system of equations

$$\sum_{j=1}^{N}\left[\frac{\delta_{kj}}{\varepsilon_j} - F_{k-j}\left(\frac{1-\varepsilon_j}{\varepsilon_j}\right)\right]\frac{Q_j}{A_j} = \sum_{j=1}^{N}\left(\delta_{kj} - F_{k-j}\right)\sigma T_j^4. \tag{A.2}$$

(A.2) relates the net energy loss (Q_j) from each surface to the temperature of each surface, where δ_{kj} is the unit tensor, σ is the Stefan-Boltzmann constant and F_{k-j} are radiation view (configuration) factors [3]. View factors for closed surfaces are defined as

$$F_{k-j} = \frac{1}{A_k}\int_{A_k}\int_{A_j}\frac{\cos\theta_k \cos\theta_j}{\pi S^2} dA_j dA_k, \tag{A.3}$$

where S is the distance from a point on surface A_j to a point on surface A_k. The angles θ_j and θ_k are measured between the line S and the normals to the surface [11]. When coupling (A.3) with heat conduction, one must apply a flux boundary condition in order to evaluate the total surface flux.

Convection

Bulk fluid elements are used as a conductive flux boundary condition to model convective heat transfer [17]. It is suitable and computationally cost effective to take this approach instead of doing full-up CFD modeled convection is not a dominant heat transfer mode for the temperature regime of interest. Specifically, we specify heat transfer on a boundary surface that can be modeled using Newton's law of cooling, which specifies that the heat flux normal to a surface q_n is proportional to the difference between the unknown temperature of the surface T and some reference temperature of the fluid in which the surface is immersed

$$q_n = h\left(T - T_r\right), \tag{A.4}$$

where h is the convection coefficient and T_r is the reference temperature [17].

Chemical Kinetics

When considering a material involving I species with J reactions, the description of the allowed reactions (stoichiometry) is given by

$$\sum_{i=1}^{I} v'_{ij}\mathscr{M}_i \rightarrow \sum_{i=1}^{I} v''_{ij}\mathscr{M}_i, \qquad j = 1,2,\ldots,J \tag{A.5}$$

where v'_{ij}, v''_{ij} are stoichiometric coefficients (usually integer values) and $\mathscr{M}$ is the chemical symbol for the ith species [31]. Stoichiometric equations are typically specified as reversible reactions, but each reaction direction is treated as an individual reaction step within this formulation. To describe global reactions, non-integer stoichiometric coefficients are used. For each step of the reaction, a reaction rate r_j, is usually defined in the form

$$r_j = k_j\left(T\right)\prod_{i=1}^{I}\left[N_i\right]^{\mu_{ij}}, \qquad j = 1,2,\ldots,J \tag{A.6}$$

where $[N_i]$ is the concentration of species i (or mole fraction) and μ_{ij} are the concentration exponents (usually $\mu_{ij} = v'_{ij}$ in kinetic theory, but here they are treated independently) [3]. Typically, the expressions for the kinetic coefficients $k_j(T)$, are given in an Arrhenius form

$$k_j\left(T\right) = T^{\beta_j}A_j \exp\left(\frac{-E_j}{RT}\right), \tag{A.7}$$

where β_j is the coefficient for a steric factor, A_j is the pre-exponential factor, E_j is the activation energy and the universal gas constant is R [38]. It is convenient to define $v_{ij} = \left(v''_{ij} - v'_{ij}\right)$, so that the change in species concentration can be described as

$$\frac{d}{dt}[N_i] = \sum_{j=1}^{J} v_{ij} r_j, \qquad i = 1, 2, \ldots, I \tag{A.8}$$

where chemical reaction process is coupled directly to the thermal diffusion problem by the volumetric source term

$$Q_r = \sum_{j=1}^{J} q_r r_j, \tag{A.9}$$

where q_j represents the known endothermic or exothermic energy release for reaction step j [14].

References

[1] Adams, B., Ebeidad, M., Eldred, M., Geraci, G., Jakeman, J., Maupin, K., Monschke, J., Swiler, L., Stephens, J., Vigil, D., Wildey, T., Bohnhoff, W., Dalbey, K., Eddy, J., Hooper, R., Hu, K., Hough, P., Ridgway, E., and Rushdi, A. "Dakota, A Multilevel Parallel Object-Oriented Framework for Design Optimization, Parameter Estimation, Uncertainty Quantification, and Sensitivity Analysis: Version 6.5 User's Manual." Technical Report SAND2014-4633, Sandia National Laboratories (2016).

[2] Carslaw, H. and Jaeger, J. *Conduction of Heat in Solids*. Oxford: Clarendon Press, 2nd edition (1959).

[3] D.K., G., Hogan, R., , and Glass, M. "COYOTE - A Finite Element Computer Program for Nonlinear Heat Conduction Problems." Technical Report SAND94-1173, Sandia National Laboratories (1994).

[4] Eldred, M., Swiler, L., and Tang, G. "Mixed aleatory-epistemic uncertainty quantification with stochastic expansions and optimization-based interval estimation." *Reliability Engineering and System Safety*, 96:1092–1113 (2011).

[5] Glass, M. "CHAPARRAL: A Library for Solving Large Enclosure Radiation Heat Transfer Problems." Technical Report SAND95-2049, Sandia National Laboratories (1995).

[6] Helton, J. "Quantification of Margins and Uncertainties: Conceptual and Computational Basis." *Reliability Engineering and System Safety*, 96:976–1013 (2011).

[7] Helton, J., Johnson, J., and Oberkampf, W. "Probability of loss of assured safety in temperature dependent systems with multiple weak and strong links." *Reliability Engineering & System Safety*, 91:320–348 (2006).

[8] Helton, J., Johnson, J., Sallaberry, C., and Storlie, C. "Survery of sampling-based methods for uncertainty and sensitivity analysis." *Reliability Engineering & System Safety*, 91:1175–1209 (2006).

[9] Helton, J. and Pilch, M. "Quantification of Margins and Uncertainties." *Reliability Engineering and System Safety*, 96:959–964 (2011).

[10] Hills, R. "Roll-up of validation results to a target application." Technical Report SAND2013-7424, Sandia National Laboratories (2013).

[11] Howell, J., Siegel, R., and Mengüç, M. *Thermal Radiation Heat Transfer*. CRC Press, 5th edition (2011).

[12] Kennedy, M. and O'Hagan, A. "Bayesian Calibration of Computer Models." *Journal of the Royal Statistics Society: Series B Statistical Methodology*, 63:425–464 (2001).

[13] Logan, R. and Nitta, C. "Comparing 10 Methods for Solution Verification, and Linking to Model Validation." Technical Report UCRL-TR-210837, Lawrence Livermore National Laboratory (2005).

[14] Mott, D., Oran, E., and van Leer, B. "A Quasi-Steady-State Solver for the Stiff Ordinary Differential Equations of Reaction Kinetics." *Journal of Computational Physics*, 164(407–428) (2000).

[15] Mullins, J. and Mahadevan, S. "Bayesian Uncertainty Integration for Model Calibration, Validation, and Prediction." *Journal of Verification, Validation and Uncertainty Quantification*, 1:011006 (2016).

[16] Newcomer, J. "A new approach to quantification of margins and uncertainties for physical simulation data." Technical Report SAND2012-7912, Sandia National Laboratories (2012).

[17] Notz, P., Subia, S., Hopkins, M., Moffat, H., and Noble, D. "Aria 1.5: User Manual." Technical Report SAND2007-2734, Sandia National Laboratories (2007).

[18] Oberkampf, W., Pilch, M., and Trucano, T. "Predictive Capability Maturity Model for Computational Modeling and Simulation." Technical Report SAND2007-5948, Sandia National Laboratories (2007).

[19] Oberkampf, W. and Roy, C. *Verification and Validation in Scientific Computing*. Cambridge, NY: Cambridge University Press (2010).

[20] Oliver, T., Malaya, N., Ulerich, R., and Moser, R. "Estimating Uncertainties in Statistics Computed from Direct Numerical Simulation." *Physics of Fluids*, 26:035101 (2014).

[21] Rebba, R., Mahadevan, S., and Huang, S. "Validation and Error Estimation of Computational Models." *Reliability Engineering and System Safety*, 91:1390–1297 (2006).

[22] Richardson, L. "The approximate arithmetical solution by finitie differences of physical problems involving differential equations, with an application to the stresses in a masonary dam." *Philosophical Transactions of the Royal Society of London: Series A, Containing Papers of a Methematical or Physical Character*, 210:307–357 (1911).

[23] Rider, W., Kamm, J., and Weirs, V. "Procedures for Calculation Verification." In *Simulation Credibility: Advances in Verification, Validation, and Uncertainty Quantification*, NASA/TP–2016-219422 and JANNAF/GL–2016-0001, technical report 2. NASA and JANNAF/GL (2016).

[24] Roache, P. *Verification and Validation in Computational Science and Engineering*. Albuquerque, NM: Hermosa Publishers (1998).

[25] Roy, C. "Review of Code and Solution Verification Procedures for Computational Simulation." *Journal of Computational Physics*, 205:131–156 (2005).

[26] Sallaberry, C. and Helton, J. "A Method of Extending the Size of Latin Hypercube Sample." In *Proceedings of the IMAC-XXIII Conference & Exposition on Structural Dynamics*, SAND2004-5092C. Orlando, FL. (2004).

[27] Saltelli, A., Ratto, M., Andres, T., Campolongo, F., Cariboni, J., Gatelli, D., Saisana, M., and Tarantola, S. *Global Sensitivity Analysis: The Primer*. West Sussex, England: John Wiley & Sons, Ltd (2008).

[28] Sankararaman, S. and Mahadevan, S. "Comprehensive framework for integration of calibration, verification, and validation." In *In: Proceedings of the 53rd AIAA/ASME/ASCE/AHS/ASC structures, structural dynamics and materials conference* (2012).

[29] Sargsyan, K., Najm, H., and Ghanem, R. "On the Statistical Calibration of Physical Models." *Internatinal Journal of Chemical Kinetics*, 47:246–276 (2015).

[30] Sierra Core Team. *Sierra Thermal/Fluids Code*. Albuquerque, NM (2017).

[31] SIERRA Thermal/Fluid Development Team. "SIERRA Multimechanics Module: Aria Theory Manual - Version 4.42." Technical Report SAND2016-10167, Sandia National Laboratories (2016).

[32] —. "SIERRA Multimechanics Module: Aria User Manual - Version 4.44." Technical Report SAND2017-3776, Sandia National Laboratories (2017).

[33] Urbina, A., Mahadevan, S., and Paez, T. "A Bayes Network Approach to Uncertainty Quantification in Hierarchically-Developed Computational Models." In *USA/South America Symposium on Stochastic Modeling and Uncertainty Quantification in Complex System* (2011).

[34] VV 10. "Guide for Verification and Validation in Computational Solid Mechanics." An American National Standard ASME V&V 10-2006, The American Society of Mechanical Engineers (2006).

[35] VV 20. "Standard for Verification and Validation in Computational Fluid Dynamics and Heat Transfer." An American National Standard ASME V&V 20-2009, The American Society of Mechanical Engineers (2009).

[36] VV/UQ and Team, C. P. "How to PIRT." Technical Report SAND2016-6465, Sandia National Laboratories (2016).

[37] —. "What is PIRT?" Technical Report SAND2016-6466, Sandia National Laboratories (2016).

[38] Young, T. "CHEMEQ - A Subroutine for Solving Stiff Ordinary Differential Equations." Technical Report NRL Memorandum Report 4091, Naval Reserach Laboratory, Washington D.C. (1980).

DISTRIBUTION:

1	MS	0828	Amalia R. Black, 01544 (electronic copy)
1	MS	0828	Brian Carnes, 01544 (electronic copy)
1	MS	0492	Kenneth C. Chen, 09411 (electronic copy)
1	MS	0828	Kevin J. Dowding, 01544 (electronic copy)
1	MS	1135	Jeffrey D. Engerer, 01532 (electronic copy)
1	MS	0836	Nicholas D. Francis, 01514 (electronic copy)
1	MS	9957	Patricia E. Gharagozloo, 08253 (electronic copy)
1	MS	0483	Carol D. Harrison, 02223 (electronic copy)
1	MS	1135	Kathryn N. G. Hoffmeister, 01532 (electronic copy)
1	MS	0825	Roy E. Hogan, Jr., 01514 (electronic copy)
1	MS	0483	Linda K. Jones, 02223 (electronic copy)
1	MS	9957	Ryan M. Keedy, 08253 (electronic copy)
1	MS	0481	James B. Milam, 02223 (electronic copy)
1	MS	0836	Brantley Mills, 01514 (electronic copy)
1	MS	1135	James T. Nakos, 01532 (electronic copy)
1	MS	0829	Justin T. Newcomer, 09136 (electronic copy)
1	MS	0836	Joe W. Shelton, 01514 (electronic copy)
1	MS	0828	Vicente J. Romero, 01544 (electronic copy)
1	MS	0386	Angel Urbina, 01544 (electronic copy)
1	MS	0483	Derek Wartman, 02223 (electronic copy)
1	MS	0828	Walter R. Witkowski, 01540 (electronic copy)
1	MS	1135	Ethan T. Zepper, 01532 (electronic copy)
1	MS	0899	Technical Library, 9536 (electronic copy)


Sandia National Laboratories